

# Forming an “Impossible” 85 solar mass Black Hole

Jorick Vink ([✉ Jorick.Vink@Armagh.ac.uk](mailto:Jorick.Vink@Armagh.ac.uk))

Armagh Observatory and Planetarium <https://orcid.org/0000-0002-8445-4397>

Erin Higgins

Armagh Observatory and Planetarium

Andreas Sander

Armagh Observatory and Planetarium

Gautham Sabhahit

Armagh Observatory and Planetarium

---

## Physical Sciences - Article

**Keywords:** 85 solar mass Black Hole, galaxy evolution, black hole masses, Cosmic time

**Posted Date:** September 28th, 2020

**DOI:** <https://doi.org/10.21203/rs.3.rs-80351/v1>

**License:**  This work is licensed under a Creative Commons Attribution 4.0 International License.

[Read Full License](#)

---

# Forming an “Impossible” 85 solar mass Black Hole

Jorick S. Vink, Erin R. Higgins, Andreas A. C. Sander, Gautham N. Sabhahit

*Armagh Observatory and Planetarium, College Hill, Armagh, BT61 9DG, Northern Ireland*

**At the end of its life, a very massive star is expected to collapse into a black hole. The masses of these black holes are pivotal for our understanding of the evolution and fate of these stars, as well as for galaxy evolution and the build-up of black hole masses through Cosmic time. The recent detection of an 85 solar mass black hole from the gravitational wave event GW 190521 appears to present a fundamental problem as to how such heavy black holes exist above the approximately 50 solar mass pair-instability limit where stars are expected to be blown to pieces with no remnant left. Here we show that for stellar models at reduced heavy element content, 90-100 solar mass stars can produce core masses sufficiently small to remain below the fundamental pair-instability limit, yet at the same time lose an amount of mass small enough to end up in an 85 solar mass black hole. A key point is that the amount of mass-loss scales with the host galaxy heavy element fraction, and not with the total amount of element enrichment that occurs naturally during the life of massive stars. Our study shows how our Universe is capable of producing heavy black holes, which are important seeds for the production of supermassive black holes that regulate the evolution of galaxies. Our evolutionary channel to the formation of an 85 solar mass black hole is of fundamental relevance for the manner in which metals are released in the outflows and explosions of the most massive stars, which is shown to be a strong function of Cosmic time.**

## 1 Introduction

The direct detection of gravitational waves from the merger of two heavy black holes (BHs) in GW 150914 confirmed one of the toughest predictions of Einstein’s Theory of general relativity. But while satisfying the world of Physics in general, for Astrophysics this was only the beginning: many were surprised by the large BH masses of respectively 36 and 29 solar masses [1], showcasing how the new field of multi-messenger Astrophysics had just re-opened the field of stellar evolution in a spectacular fashion. Stellar-mass black holes had previously been revealed by their interaction in binary systems [25], but the maximum BH mass in our Milky Way is not higher than roughly 15 times the mass of the Sun [6]. While we know that very massive stars (VMS) above 100 solar masses exist [34], this mass is significantly diminished via stellar winds throughout their entire evolution [33]. The BH ‘obesity’ measured by LIGO/VIRGO therefore supported the assumption that the gravitational wave event occurred in a part of the Universe still pristine in its enrichment with heavy elements (“metallicity”), lowering stellar wind mass loss [31]. This ‘pristine’ solution was widely accepted until the announcement of the formation of a heavy black hole of order 70 solar masses in LB-1 in the Milky Way [20], spurring stellar evolution theorists to avoid heavy mass loss in the Milky Way [5, 15], either by arbitrarily lowering the mass-loss rates of VMS – seemingly contradicting VMS mass-loss calibrations [33] – or by invoking the presence of a strong dipolar magnetic field that could quench the wind [27]. While magnetic fields in some 5-10% of massive OB stars do indeed exist, no fields have yet been detected in VMS [4]. The problem of the formation of a  $70 M_{\odot}$  BH in a solar-metallicity environment apparently resolved itself when the spectral signatures of LB-1 were re-interpreted [3].

The recent discovery of GW 190521, involving the merger of a 85 solar mass and 66 solar mass BH, is not only record-breaking in terms of obtained BH masses, but also represents an exciting challenge. The masses of both black holes in GW 190521 are in the limits of what is called the second<sup>1</sup> mass gap between approx. 50-130 solar masses, where stars cannot collapse into BHs due to pair instability resulting from electron-positron pair production [13].

Beside a regime where the whole star is disrupted by a so-called pair-instability supernova [PISN, see e.g. 19], there is also a regime where electron-positron pair production does not disrupt the star as whole, but causes significant violent pulses leading to enhanced mass loss before an eventual “pulsational pair-instability supernova” [PPISN 35]. In contrast to PISNe, PPISNe are leading to a BH as there is a remaining iron core that collapses. Still, the pulses before the eventual collapse remove so much mass, that both PISNe and PPISNe lead to a significant “forbidden” mass regime, where no first-generation heavy black holes should be found. The lower boundary of this regime is commonly assumed to be at 40-50 solar masses. [11, 36]. Given inherent uncertainties, it is mainly the  $85 M_{\odot}$  BH in GW 190521 that surprised the Astronomical community and led to the speculation that such heavy BHs of up to 85 solar masses are most likely ”second generation” BHs, implying they must have merged from lighter BHs in an earlier event [2]. The preferred solutions involve mergers of lower-mass BHs or stars in dense cluster/galactic environments [14, 28], however as *both* BHs in the system are above the 40-50 solar mass boundary, this would imply an arguably contrived situation involving at least 2 double mergers, i.e. at least involving 4 objects. While one cannot rule out such a scenario, we will show that the formation of massive BH on

---

<sup>1</sup>The first mass gap refers to a observational gap between the most massive neutron stars and 'lightest' black holes

the order of  $85 M_{\odot}$  does neither require an earlier BH merger nor more exotic scenarios such as a modified gravitation theory [21]. Instead, our uncertain understanding of the evolution of (very) massive stars due to our limited knowledge of wind mass loss has lead to an underestimating of the lower boundary of the second mass gap at low metallicity ( $Z$ ).

In the following, we will show that at low, but not necessarily zero metallicity, stars on the order of 90 solar masses can retain most of their hydrogen envelope and avoid the pair-instability regime. By critically assessing stellar wind mass loss and avoiding the high heavy element content seen in the solar neighborhood, we will find a stellar evolution solution for what has been considered an “impossible” BH mass.

## 2 Evolution of very massive stars

The aim is to show that a VMS of order 100 solar masses can loose little mass at low  $Z$  to have a sufficient total mass to make a first generation BH of order 85 solar masses. At the same time, our models need to avoid too high CO core masses as otherwise pair production during oxygen burning might produce pulses that potentially remove too much mass. We refer to this as the critical limit.

The obvious way to remain below the critical boundary is to start off with an initial mass that is comparatively low, as more massive stars have larger and larger convective cores [7, 18, 34]. An accompanying ingredient is to keep the amount of core overshooting under control by not unnecessarily applying large core overshooting [17]. We therefore employ a small amount of overshooting as is common in massive star evolution [9].

**Stellar evolution modelling** After describing our strategy above, we avail of the MESA [26] stellar evolution code and evolve the objects at least through core oxygen burning, and check if they encounter pair instability (PI). Convection is treated using the standard mixing length theory ( $\alpha_{\text{MLT}} = 1.5$ ), with extra convective mixing above the H-burning core by so-called “step-overshooting” ( $\alpha_{\text{ov}} = 0.1$ ). Rotation is implemented with  $\Omega/\Omega_{\text{crit}} = 0.2$ , and rotational mixing instabilities are included [16]. In order to evolve pre-core-collapse supernova models at these high initial masses, we have used the MLT++ option in MESA which increases the transport of convective energy in low density envelopes.

Figure 1 showcases the stellar structure as a function of evolutionary timescale (“Kippenhahn diagram”) of a  $90 M_{\odot}$  star at  $0.1 Z_{\odot}$ . This model eventually collapses into a BH of about  $80 M_{\odot}$ . This model, Model 1, evolves through all stages up to Si burning with a final CO core mass of  $38 M_{\odot}$ . At this point, the star retains a massive, H-rich envelope of  $36 M_{\odot}$ , making it almost as large as the CO core. In contrast to recent calculations determining the maximum BH mass below the pair instability gap [11, 36], we do not a priori assume that stars forming heavy BHs must have lost their outer envelope. Instead, we have critically analysed the treatment of mass loss employed in massive star evolution codes such as MESA and identified major caveats, which effectively lead to high mass-loss during core helium (He) burning. The removal of these ingredients, which are not sufficient at low  $Z$  is the prime reason why our Model 1 yields a massive BH.

To demonstrate this, we have calculated a model with the same initial mass and metallicity using the standard MESA treatment (Model 2; see Fig. 2). The larger core mass of Model 2 leads to

pair instability, thus constraining the initial stellar mass for BH formation below the second mass gap. Similarly, due to the higher initial mass of  $100 M_{\odot}$  in Model 3 at lower  $Z$  ( $0.01 Z_{\odot}$ ), the final core mass leads to pair instability. While for the same initial parameters in Model 4 as in Model 1, except for lower  $Z$ , a BH of  $88 M_{\odot}$  is formed.

As stellar mass is the prime quantity for stellar evolution, the loss of mass due to stellar wind is a highly important ingredient in massive star evolution. The determination of wind mass loss is complex and can as yet not be performed self-consistently during stellar evolution. Therefore, evolution models rely on prescribed theoretical or empirical formulae or "recipes" for specific temperature ( $T_{\text{eff}}$ ) regimes. The application of such recipes beyond the validity regime where they were established has to be carefully considered as inadequate extrapolations may lead to over- or underestimations of orders of magnitude [30].

A standard treatment inherent to various stellar evolution a collection of three different mass-loss recipes, which is referred to as the "Dutch wind recipe" in MESA: one formulae describes hot star winds [32], while a distinct formula is used for dust-driven cool star winds [8]. For stars which had their H outer envelope removed a third formula is usually employed. In MESA, this [23] relation is based on an empirical study of Wolf-Rayet stars in the Milky Way.

Figure 3 shows that in the standard MESA wind treatment, there is rapid envelope loss during core He-burning, even at low  $Z$ . The reason for the strong mass loss in this Model 2 is that the code has switched from the hot-star recipe [32] to the one for cool stars [8]. The mass-loss description for the cool star regime is employed to describe dusty red supergiants, which have

temperatures of just 3000-4000 K. As the switch occurs at 10000 K, but the blue-yellow supergiants in this temperature range (8 000-12 000 K) are too hot to form dust, the winds are expected to be driven by iron-dominated gas opacities rather than dust. Consequentially, despite uncertainty about the mass loss in this blue-yellow temperature regime due to iron ionization changes [32], the utilization of these far lower mass-loss rates is considered far more physical. As all our model stars are blue-yellow supergiants and avoid the regime of red supergiants, we obtain the dramatic difference depicted in Fig. 3, where we show that low  $Z$  stars can retain a considerably larger fraction of their H envelope (Model 1) than using the canonical "Dutch" treatment (Model 2).

Another aspect inherent to evolution modelling with evolution codes such as MESA is the switch to a third formula. Intended to describe the mass loss of He-enriched Wolf-Rayet stars [23], it is applied to evolved stars above 10 000 K. As the mass loss scales with iron content, but not with metals that can be produced via self-enrichment such as CNO [29, 31], we apply the physically motivated standard hot star wind treatment [32] also for our evolved models as a Wolf Rayet-like treatment would yet again lead to artificially high mass-loss rates at low  $Z$ .

**The silent collapse of the star** The core collapse of a massive star is not necessarily accompanied by a supernova explosion. Instead, massive stars below the (pulsation) pair-instability regime are mostly likely to produce an immediate black hole – a so-called “failed supernova” – if their core is compact enough [10, 24]. A common measurement for the core compactness is the parameter

$$\xi_{2.5} = \frac{2.5}{r(M = 2.5M_\odot)[1000 \text{ km}]} \quad (1)$$

Our models avoiding pair instability have values of 0.33 (model 1,  $0.1 Z_{\odot}$ ) and 0.55 (model 4,  $0.01 Z_{\odot}$ ). While the lower boundary of  $\xi_{2.5}$  for a failed supernova is still a matter of debate [10], model 4 is safely above even the larger estimates. The value for Model 1 is likely underestimated as this model is stopped at Si burning, but even a compactness of 0.3 could be sufficient to avoid a supernova according to newer studies [22].

Besides the collapse of the whole core without a supernova, also the outer layers of the star have to fall into the newly formed BH in order to reach the high masses observed in recent GW events. To avoid a significant ejection of mass at core collapse, therefore not only the core, but also the envelope needs to be sufficiently compact. We thus consider the envelope compactness parameter [12]

$$\xi_{\text{env}} = \frac{M_{\text{f}}[M_{\odot}]}{R_{\text{f}}[M_{\odot}]} \quad (2)$$

with  $M_{\text{f}}$  and  $R_{\text{f}}$  denoting the total mass and radius of the star at core collapse. At the time of core collapse, our model stars will appear as blue supergiants, for which  $\xi_{\text{env}}$  has to be higher than 0.5 to avoid any mass ejection [12]. This is fulfilled for our model 4 ( $\xi_{\text{env}} = 0.86$ ) calculated at  $0.01 Z_{\odot}$ . Based on recent simulations for ejecta masses in failed supernovae [12], our model 1 (a blue supergiant, see Fig. 2) at  $0.1 Z_{\odot}$  ( $\xi_{\text{env}} = 0.21$ ) will not lose much mass either ( $M_{\text{ej}} < 0.2 M_{\odot}$ ) as failed supernovae only yield large ejecta masses for red supergiants where the outer layers are very weakly bound to the star at all. Hence, even at  $0.1 Z_{\odot}$  our evolution model is able to produce a black hole of about  $80 M_{\odot}$ .

### 3 Outlook

In our pilot study we find BH masses in the range of 80-90  $M_{\odot}$  for  $Z$  between 1% and 10% of the solar value. While detailed studies involving full stellar evolution grids are planned to finalize the input physics and exact  $Z$ -dependent boundaries between BH formation and pair instability, we can confidently predict that the maximum BH to be on the order of 90  $M_{\odot}$  at low  $Z$  (below 10% solar  $Z$ ). Our predictions on the maximum BH mass are based on evolution models with  $M_{\text{init}} \sim 90$ - $100 M_{\odot}$  in the 0.01 - 0.1  $Z_{\odot}$  range. At the highest considered metallicity, we find an optimum situation producing an 80  $M_{\odot}$  BH while barely avoiding pair instability, allowing us to constrain the upper stellar mass limit as well as upper  $Z$ -limit for *first generation* BH formation. At larger  $Z$ , enhanced wind mass loss will rapidly drop the maximum BH limit down to the established value of about 50  $M_{\odot}$ .

Consequently, the BH masses derived from gravitational wave events with observatories such as LIGO/VIRGO need to be interpreted in the context of their host  $Z$  environment. While this will be rather challenging to determine for most events in the near future, it underlines the desire to electromagnetic follow-up searches of gravitational wave events. Only for a certain range of masses between approximately 90 and 130  $M_{\odot}$ , first generation black holes can be ruled out independent of  $Z$  based on our physically motivated evolution modelling.

The conservation of large H-envelopes in VMS at low  $Z$  has direct implications for stellar yield predictions, in particular when the entire star collapses into a heavy BH and only a tiny fraction of heavy elements is returned to the interstellar medium. As our model stars stay “blue” ,

implying their radial extension is relatively modest in comparison to those of red supergiants, this may limit the interaction frequency with potential binary companions. Still, there will be situations where binary companions remove parts of the envelope, leading to higher metal yields, and lower BH masses. The heavy black holes obtained in recent GW events such as GW 150921 show that wind mass loss at low  $Z$  is a crucial ingredient that needs to be carefully considered in stellar evolution and population synthesis modelling to avoid blurring our perception of how the Universe evolved into what we see today.

From the analysis and modelling performed here, we may already confidently conclude that for low- $Z$  host galaxies it is possible to create *first generation* BHs up to values as large as  $\sim 90 M_{\odot}$ , without the need to invoke *second generation* BH formation, extreme assumptions, or exotic physics.

Author contributions. All authors were involved in both the research and writing of the Manuscript.

1. B. P. Abbott, R. Abbott, T. D. Abbott, LIGO Scientific Collaboration, and Virgo Collaboration. Astrophysical Implications of the Binary Black-hole Merger GW150914. *ApJ*, 818(2):L22, February 2016.
2. R. Abbott, T. D. Abbott, S. Abraham, LIGO Scientific Collaboration, and Virgo Collaboration. Properties and Astrophysical Implications of the  $150 M_{\odot}$  Binary Black Hole Merger GW190521. *ApJ*, 900(1):L13, September 2020.

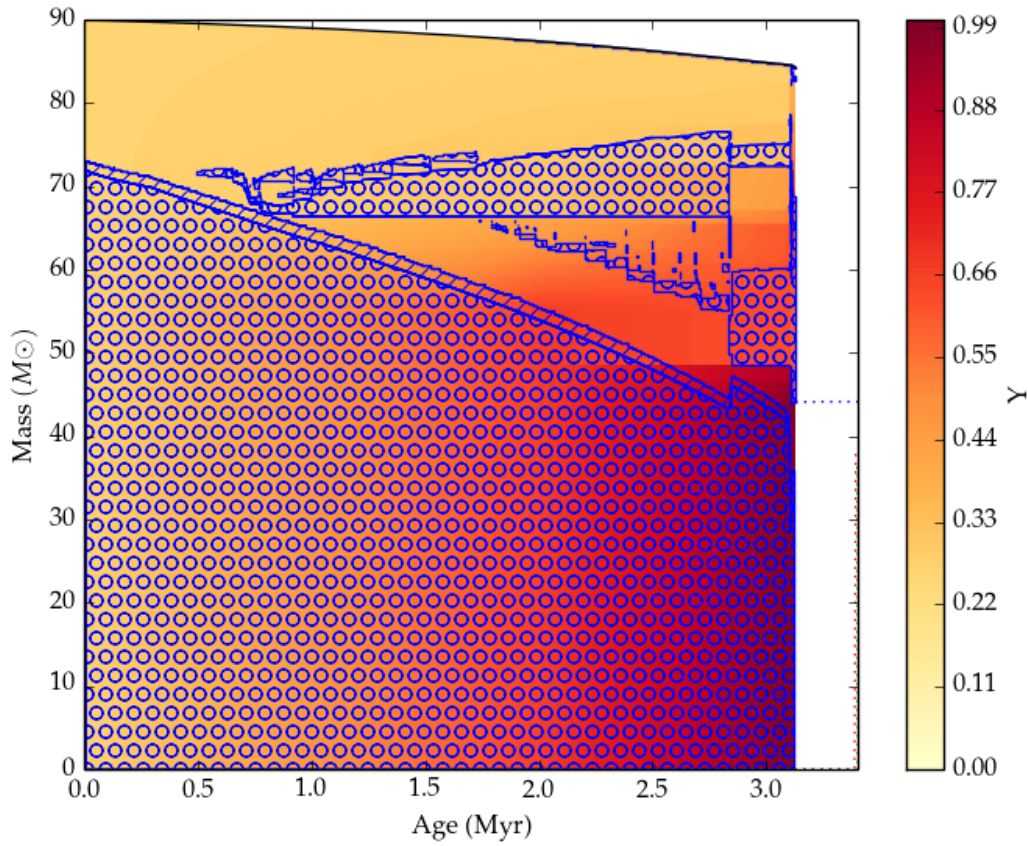


Figure 1: Evolution of the internal structure of our model 1 with initial mass  $90 M_{\odot}$  and metallicity  $0.1 Z_{\odot}$ , as a function of mass ( $M_{\odot}$ ) and stellar age (Myrs). The colour bar represents the core Helium abundance while blue circles illustrate convective zones. The hatched blue region denotes the small overshooting layer above the H-burning core. The dashed blue line at 3Myrs shows the final core mass.

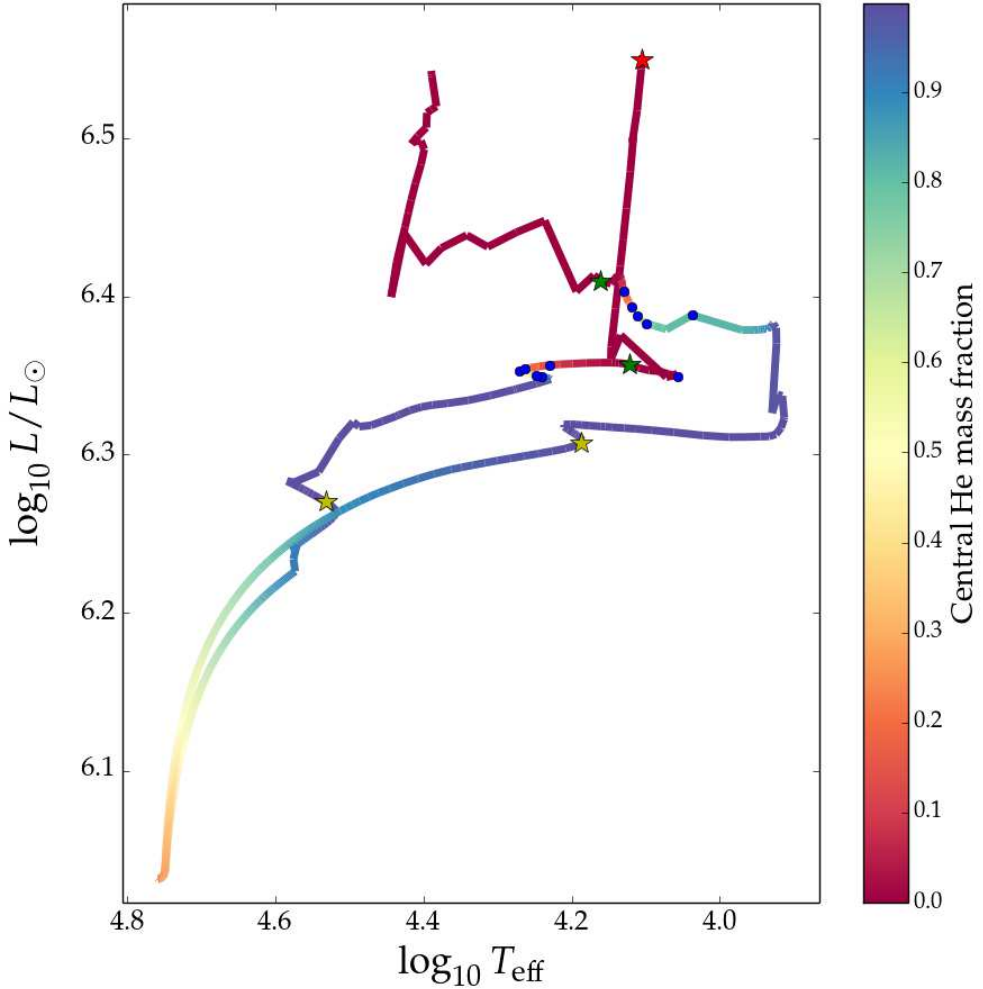


Figure 2: Comparison of model 1 and model 2 in a Hertzsprung-Russell diagram. The colour bar represents the core He abundance, with yellow stars showing the TAMS position, green stars illustrating the end of core He-burning, and red stars showing the end of core O-burning. Note that Model 2 does not reach the end of core O-burning. Blue dots show time-steps of 50,000 years after core H exhaustion, where time is spent as a blue supergiant (i.e. above  $\log T_{\text{eff}} > 3.65$ ).

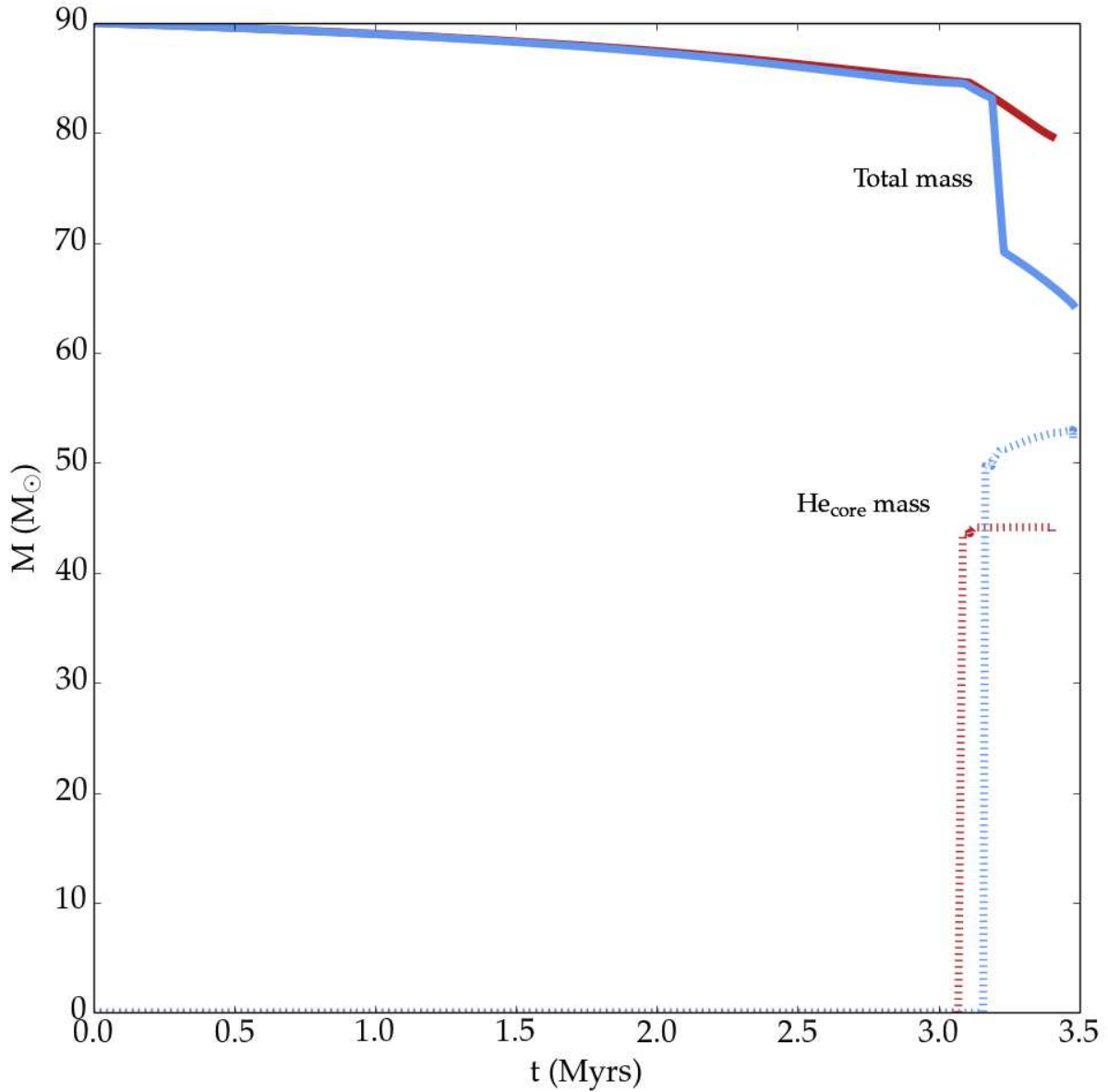


Figure 3: Total (solid) and He-core (dashed) masses as a function of time (Myrs). Red lines show model 1, where we have corrected mass-loss rates with Z-scaling from [31]. Blue lines show model 2, as a comparison to our working model, with standard 'Dutch' mass loss.

3. Michael Abdul-Masih, Gareth Banyard, Julia Bodensteiner, Emma Bordier, Dominic M. Bowman, Karan Dsilva, Matthias Fabry, Calum Hawcroft, Laurent Mahy, Pablo Marchant, Gert Raskin, Maddalena Reggiani, Tomer Shenar, Andrew Tkachenko, Hans Van Winckel, Lore Vermeylen, and Hugues Sana. On the signature of a 70-solar-mass black hole in LB-1. *Nature*, 580(7805):E11–E15, April 2020.
4. S. Bagnulo, G. A. Wade, Y. Nazé, J. H. Grunhut, M. E. Shultz, D. J. Asher, P. A. Crowther, C. J. Evans, A. David-Uraz, I. D. Howarth, N. Morrell, M. S. Munoz, C. Neiner, J. Puls, M. K. Szymański, and J. S. Vink. A search for strong magnetic fields in massive and very massive stars in the Magellanic Clouds. *A&A*, 635:A163, March 2020.
5. K. Belczynski, R. Hirschi, E. A. Kaiser, Jifeng Liu, J. Casares, Youjun Lu, R. O’Shaughnessy, A. Heger, S. Justham, and R. Soria. The Formation of a  $70 M_{\odot}$  Black Hole at High Metallicity. *ApJ*, 890(2):113, February 2020.
6. Krzysztof Belczynski, Tomasz Bulik, Chris L. Fryer, Ashley Ruiter, Francesca Valsecchi, Jorick S. Vink, and Jarrod R. Hurley. On the Maximum Mass of Stellar Black Holes. *ApJ*, 714(2):1217–1226, May 2010.
7. Paul A. Crowther, Olivier Schnurr, Raphael Hirschi, Norhasliza Yusof, Richard J. Parker, Simon P. Goodwin, and Hasan Abu Kassim. The R136 star cluster hosts several stars whose individual masses greatly exceed the accepted  $150 M_{\text{solar}}$  stellar mass limit. *MNRAS*, 408(2):731–751, October 2010.

8. C. de Jager, H. Nieuwenhuijzen, and K. A. van der Hucht. Mass loss rates in the Hertzsprung-Russell diagram. *A&AS*, 72:259–289, February 1988.
9. S. Ekström, C. Georgy, P. Eggenberger, G. Meynet, N. Mowlavi, A. Wyttenbach, A. Granada, T. Decressin, R. Hirschi, U. Frischknecht, C. Charbonnel, and A. Maeder. Grids of stellar models with rotation. I. Models from 0.8 to 120 M at solar metallicity ( $Z = 0.014$ ). *A&A*, 537:A146, January 2012.
10. T. Ertl, H. Th. Janka, S. E. Woosley, T. Sukhbold, and M. Ugliano. A Two-parameter Criterion for Classifying the Explodability of Massive Stars by the Neutrino-driven Mechanism. *ApJ*, 818(2):124, February 2016.
11. R. Farmer, M. Renzo, S. E. de Mink, P. Marchant, and S. Justham. Mind the Gap: The Location of the Lower Edge of the Pair-instability Supernova Black Hole Mass Gap. *ApJ*, 887(1):53, December 2019.
12. Rodrigo Fernández, Eliot Quataert, Kazumi Kashiyama, and Eric R. Coughlin. Mass ejection in failed supernovae: variation with stellar progenitor. *MNRAS*, 476(2):2366–2383, May 2018.
13. William A. Fowler and F. Hoyle. Neutrino Processes and Pair Formation in Massive Stars and Supernovae. *ApJS*, 9:201, December 1964.
14. Giacomo Fragione, Abraham Loeb, and Frederic A. Rasio. On the Origin of GW190521-like events from repeated black hole mergers in star clusters. *arXiv e-prints*, page arXiv:2009.05065, September 2020.

15. Jose H. Groh, Eoin J. Farrell, Georges Meynet, Nathan Smith, Laura Murphy, Andrew P. Allan, Cyril Georgy, and Sylvia Ekstroem. Massive Black Holes Regulated by Luminous Blue Variable Mass Loss and Magnetic Fields. *ApJ*, 900(2):98, September 2020.
16. A. Heger, N. Langer, and S. E. Woosley. Presupernova Evolution of Rotating Massive Stars. I. Numerical Method and Evolution of the Internal Stellar Structure. *ApJ*, 528(1):368–396, January 2000.
17. Erin R. Higgins and Jorick S. Vink. Theoretical investigation of the Humphreys-Davidson limit at high and low metallicity. *A&A*, 635:A175, March 2020.
18. K. Köhler, N. Langer, A. de Koter, S. E. de Mink, P. A. Crowther, C. J. Evans, G. Gräfener, H. Sana, D. Sanyal, F. R. N. Schneider, and J. S. Vink. The evolution of rotating very massive stars with LMC composition. *A&A*, 573:A71, January 2015.
19. N. Langer, C. A. Norman, A. de Koter, J. S. Vink, M. Cantiello, and S. C. Yoon. Pair creation supernovae at low and high redshift. *A&A*, 475(2):L19–L23, November 2007.
20. Jifeng Liu, Haotong Zhang, and Andrew W. et al. Howard. A wide star-black-hole binary system from radial-velocity measurements. *Nature*, 575(7784):618–621, November 2019.
21. J. W. Moffat. Modified Gravitation Theory (MOG) and the aLIGO GW190521 Gravitational Wave Event. *arXiv e-prints*, page arXiv:2009.04360, September 2020.
22. Bernhard Müller, Alexander Heger, David Liptai, and Joshua B. Cameron. A simple approach to the supernova progenitor-explosion connection. *MNRAS*, 460(1):742–764, July 2016.

23. T. Nugis and H. J. G. L. M. Lamers. Mass-loss rates of Wolf-Rayet stars as a function of stellar parameters. *A&A*, 360:227–244, August 2000.
24. Evan O’Connor and Christian D. Ott. Black Hole Formation in Failing Core-Collapse Supernovae. *ApJ*, 730(2):70, April 2011.
25. Jerome A. Orosz, Jeffrey E. McClintock, Jason P. Aufdenberg, Ronald A. Remillard, Mark J. Reid, Ramesh Narayan, and Lijun Gou. The Mass of the Black Hole in Cygnus X-1. *ApJ*, 742(2):84, December 2011.
26. Bill Paxton, Josiah Schwab, Evan B. Bauer, Lars Bildsten, Sergei Blinnikov, Paul Duffell, R. Farmer, Jared A. Goldberg, Pablo Marchant, Elena Sorokina, Anne Thoul, Richard H. D. Townsend, and F. X. Timmes. Modules for Experiments in Stellar Astrophysics (MESA): Convective Boundaries, Element Diffusion, and Massive Star Explosions. *ApJS*, 234(2):34, February 2018.
27. V. Petit, Z. Keszthelyi, R. MacInnis, D. H. Cohen, R. H. D. Townsend, G. A. Wade, S. L. Thomas, S. P. Owocki, J. Puls, and A. ud-Doula. Magnetic massive stars as progenitors of ‘heavy’ stellar-mass black holes. *MNRAS*, 466(1):1052–1060, April 2017.
28. Isobel M. Romero-Shaw, Paul D. Lasky, Eric Thrane, and Juan Calderon Bustillo. GW190521: orbital eccentricity and signatures of dynamical formation in a binary black hole merger signal. *arXiv e-prints*, page arXiv:2009.04771, September 2020.
29. Andreas A. C. Sander, J. S. Vink, and W. R. Hamann. Driving classical Wolf-Rayet winds: a  $\Gamma$ - and Z-dependent mass-loss. *MNRAS*, 491(3):4406–4425, January 2020.

30. Andreas A. C. Sander and Jorick S. Vink. On the nature of massive helium star winds and Wolf-Rayet-type mass loss. *arXiv e-prints*, page arXiv:2009.01849, September 2020.
31. Jorick S. Vink and A. de Koter. On the metallicity dependence of Wolf-Rayet winds. *A&A*, 442(2):587–596, November 2005.
32. Jorick S. Vink, A. de Koter, and H. J. G. L. M. Lamers. Mass-loss predictions for O and B stars as a function of metallicity. *A&A*, 369:574–588, April 2001.
33. Jorick S. Vink and Götz Gräfener. The Transition Mass-loss Rate: Calibrating the Role of Line-driven Winds in Massive Star Evolution. *ApJ*, 751(2):L34, June 2012.
34. Jorick S. Vink, Alexander Heger, Mark R. Krumholz, Joachim Puls, S. Banerjee, N. Castro, K. J. Chen, A. N. Chenè, P. A. Crowther, A. Daminelli, G. Gräfener, J. H. Groh, W. R. Hamann, S. Heap, A. Herrero, L. Kaper, F. Najarro, L. M. Osokinova, A. Roman-Lopes, A. Rosen, A. Sander, M. Shirazi, Y. Sugawara, F. Tramper, D. Vanbeveren, R. Voss, A. Wofford, and Y. Zhang. Very Massive Stars in the local Universe. *Highlights of Astronomy*, 16:51–79, March 2015.
35. S. E. Woosley. Pulsational Pair-instability Supernovae. *ApJ*, 836(2):244, February 2017.
36. S. E. Woosley, Tuguldur Sukhbold, and H. T. Janka. The Birth Function for Black Holes and Neutron Stars in Close Binaries. *ApJ*, 896(1):56, June 2020.

Model	$Z/Z_{\odot}$	$M_{\text{init}}$	$M_f$	$M_{\text{env}}$	$M_{\text{CO}}$	
1	0.1	90	79.66	36.29	37.97	core collapse
2	0.1	90	64.37	12.40	42.98	pair instability
3	0.01	100	95.98	29.99	57.95	pair instability
4	0.01	90	88.17	38.40	49.20	core collapse

Table 1: Fundamental parameters of our benchmark models, including the initial metallicity  $Z$  and mass  $M_{\text{init}}$ . For all models, we also list the total mass  $M_f$ , envelope mass  $M_{\text{env}}$ , and CO core mass  $M_{\text{CO}}$  of the final model stage. Models which are subject to pair instability were stopped at this point.

# Figures

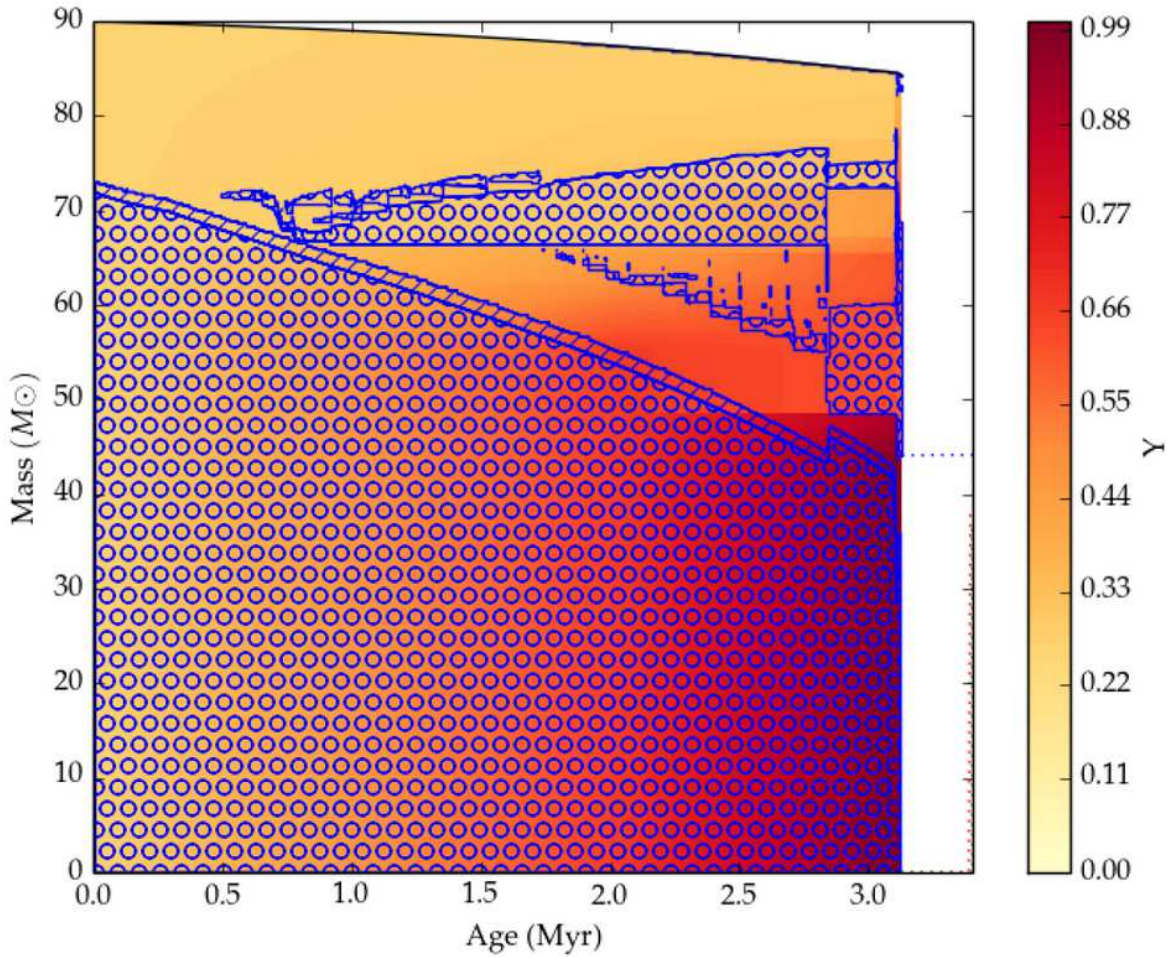


**Figure 1**

Evolution of the internal structure of our model 1 with initial mass  $90M_{\odot}$  and metallicity  $0.1Z_{\odot}$ , as a function of mass ( $M_{\odot}$ ) and stellar age (Myrs). The colour bar represents the core Helium abundance while blue circles illustrate convective zones. The hatched blue region denotes the small overshooting layer above the H-burning core. The dashed blue line at 3Myrs shows the final core mass.

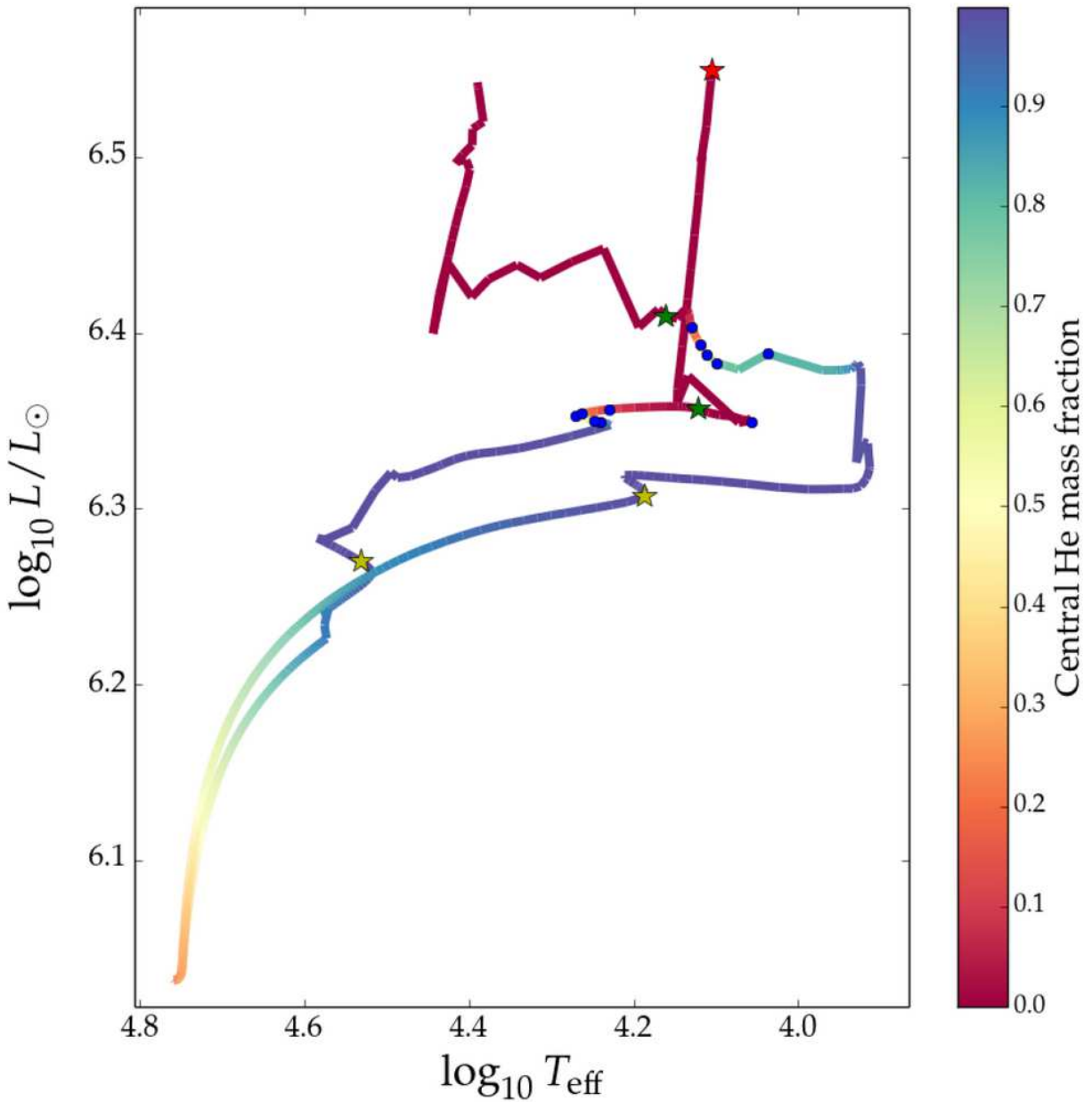


**Figure 2**

Comparison of model 1 and model 2 in a Hertzsprung-Russell diagram. The colour bar represents the core He abundance, with yellow stars showing the TAMS position, green stars illustrating the end of core He-burning, and red stars showing the end of core O-burning. Note that Model 2 does not reach the end of core O-burning. Blue dots show time-steps of 50,000 years after core H exhaustion, where time is spent as a blue supergiant (i.e. above  $\log \text{Teff} > 3.65$ ).

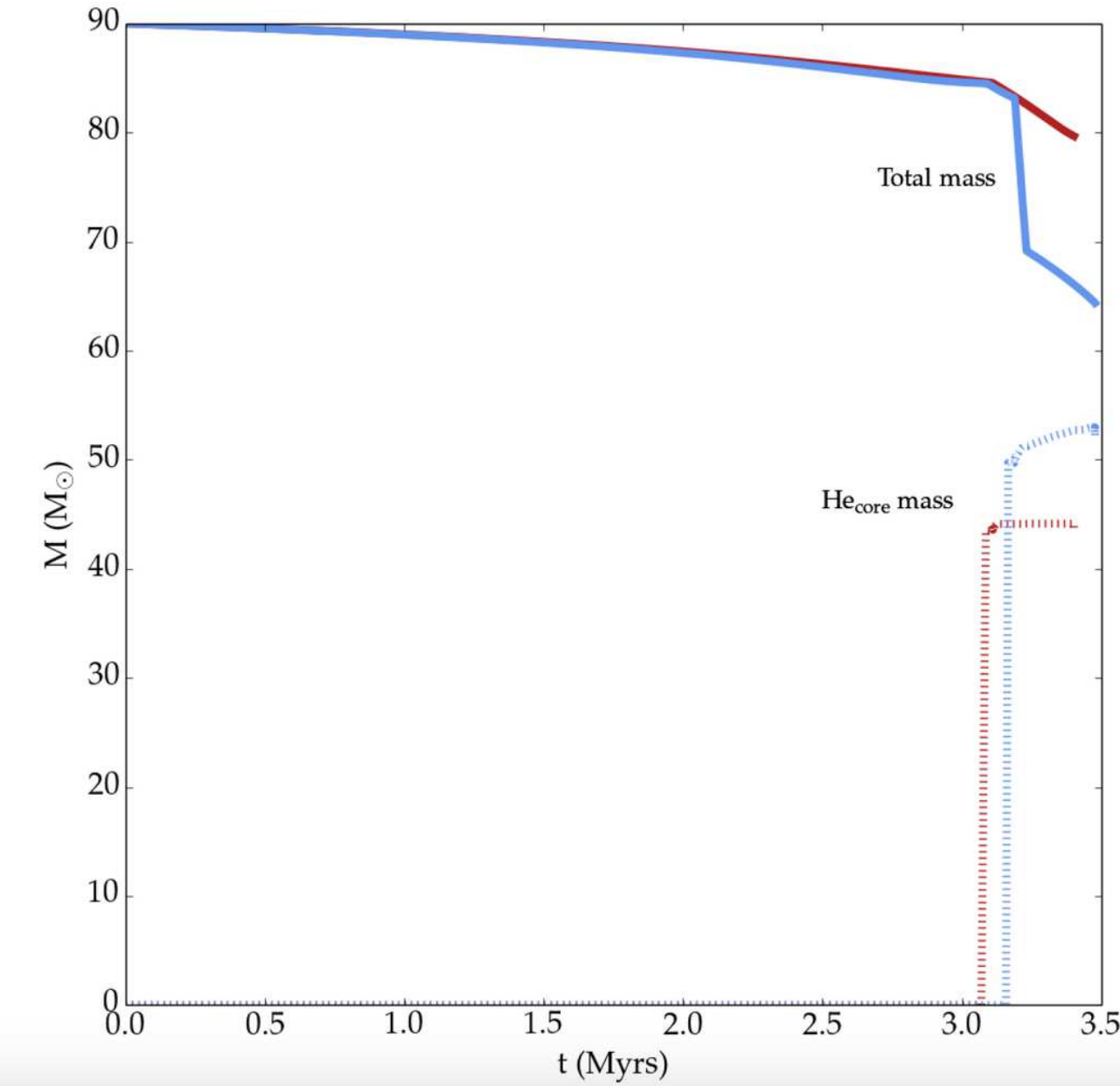


**Figure 3**

Total (solid) and He-core (dashed) masses as a function of time (Myrs). Red lines show model 1, where we have corrected mass-loss rates with Z-scaling from [31]. Blue lines show model 2, as a comparison to our working model, with standard 'Dutch' mass loss.